

## N O T I C E

THIS DOCUMENT HAS BEEN REPRODUCED FROM  
MICROFICHE. ALTHOUGH IT IS RECOGNIZED THAT  
CERTAIN PORTIONS ARE ILLEGIBLE, IT IS BEING RELEASED  
IN THE INTEREST OF MAKING AVAILABLE AS MUCH  
INFORMATION AS POSSIBLE

**NASA CR-166631**

UCBSSL Series 21 Issue 7

Instrumentation Development for the EUVE

NAS 5-24445

Report #9

Feb. 15, 1980 - May 15, 1980

Prepared June 2, 1980



Prepared by

*David Finley*  
David Finley

Approved by

*Stuart Bowyer*  
Stuart Bowyer  
Principal Investigator

Space Sciences Laboratory  
University of California  
Berkeley, California 94720

(NASA-CR-166631) INSTRUMENTATION  
DEVELOPMENT FOR THE EUVE Progress Report,  
15 Feb. - 15 May 1980 (California Univ.)  
34 p HC A03/MF A01 CSCL 20F

N81-18851

Unclas  
G3/74 16537

## I. INTRODUCTION

This progress report for NASA contract NAS 5-24445 covers the period 15 February to 15 May 1980. Work is currently going forward on several fronts: The prototype mirror was successfully replated with a thick layer of nickel and diamond turned again. A comprehensive study was made of optimizing the sensitivity of the instrumnets, depending on the filter material, and on the available telemetry. A critical analysis has been carried out of the JHU Preliminary Project Definition Document. We have submitted to JPL an updated description of the instrument papameters for the Explorer satellite. Further studies of the electron cloud distribution produced by a channel plate have been done, and a wedge and strip anode with 17 quartets per inch was shown to image with better than 0.5% linearity. Half the microchannel plates being used in the lifetest have been through initial processing and are now in the lifetest vacuum chamber.

## II. SUMMARY OF STATUS

TASK	DESCRIPTION	STATUS	
		Previous reporting period	Current reporting period
1	<u>Optical Technology</u>		
1-1	Performance Requirements	Completed	Completed
1-2	Sample Evaluation	Completed	Completed
1-3	Design Proto-optic	Completed	Completed
1-4	Procure Proto-optic	Second diamond turning in progress	Second diamond turning completed
1-5	Evaluation	In progress	In progress
1-6	Environmental Testing	TBD	TBD
2	<u>Image System Tradeoffs</u>		
2-1	Field of View Optimization	Completed	Completed
2-2	Spin-rate Dependence	Completed	Completed
2-3	Update EUV Background	In progress	In progress
2-4	Review RFP	In progress	Completed
3	<u>Detector Development</u>		
3-1	Alternative Process Development	In progress	In progress
3-2	Specification and Procedure Definition	Completed	Completed
3-3	Procurement	Completed	Completed
3-4	Test and Evaluation	In progress	In progress
3-5	Environmental Testing	TBD	TBD
3-6	Evaluate Redundant Configuration	In progress	Completed
4	<u>Actuator Mechanisms</u>		
4-1	Design	Completed	Completed
4-2	Fabrication	Completed	Completed
4-3	Evaluation	In progress	In progress

Summary of Status, cont.

TASK	DESCRIPTION	STATUS	
		Previous reporting period	Current reporting period
5	<u>Filter Development</u>		
5-1	Procurement	Completed	Completed
5-2	Evaluation	In progress	Completed
6	<u>Processing Electronics</u>		
6-1	Design	Completed	Completed
6-2	Procurement	Completed	Completed
6-3	Breadboard Checkout	In progress	In progress
6-4	Environmental Evaluation	TBD	TBD

### III. TASK 1 OPTICAL TECHNOLOGY

Prototype Optics Fabrication -- The mirror was replated with 0.005" of electroless nickel, and was diamond turned again, and optically tested. The diamond turning was not without its difficulties. Unlike the aluminum, the nickel caused tool chatter when it was first attempted to machine the bore of the mirror. We then placed large springs wrapped around the outer perimeter of the piece, which succeeded in almost completely damping out the chatter. We then proceeded with the diamond turning, which went smoothly thereafter. The mirror was then optically tested. The figure was as good as before, and the mirror imaged well. The only difference from the diamond turned aluminum surface was that the nickel has somewhat more pronounced residual tool marks, resulting in visible diffraction from the surface. However, these tool marks will cause no problem for the polishing phase, where the main problem is removal of the ripples of up to an inch in wavelength. The polishing will begin shortly.

### IV. TASK 2 IMAGE SYSTEM TRADEOFFS

Optimization of Telemetry Rate -- In the process of optimizing the complement of filters, it became clear that a definitive study was necessary to determine the effects of telemetry on sensitivity. A comprehensive study of this matter is now under way and will be reported on as part of the next quarterly report. A preliminary conclusion is that the Al/C filter, representing the most important EUV bandpass from 150 - 350 Å, is in a telemetry limited regime. That is, its sensitivity is increased by the square root of the factor by which the telemetry is increased. The other filters are also helped by a gain in telemetry.

Spin Rate, Telemetry, etc. -- APL produced a proposal regarding spacecraft design parameters, some of which might have an adverse impact on the useful scientific return from this mission. We prepared a critique of the salient points, including the relation between data rate, spin rate, and downlinking capabilities. A detailed report is included as Appendix I.

#### V. TASK 3 DETECTOR DEVELOPMENT

MCP's and Anodes -- We have remeasured the spatial distribution of the charge cloud exiting the rear of a chevron pair. The cloud has a FWHM of 1.46 mm at a MCP to anode spacing of 6 mm, with a -300V bias. This is smaller than that given by the previous less accurate measurement, and confirmed the need for a denser wedge and strip array in order to achieve good linearity. The original anode, with 4.2 mm per quartet, did not function properly. Guided by the new data, the anode was reduced by a factor of 3, giving 1.4 mm per quartet, and the resultant nonlinearity at 1 cm spacing was less than 0.5%. A new anode, with 1 mm per quartet, and requiring no through holes, is being developed. This will be a 1" x 1" prototype, and if it works out as anticipated, some full 3" x 3" anodes will be built. Reports on both the charge cloud size and on anode development will be included in the next quarterly report.

MCP Life Test -- The lifetest facility is currently in operation with about half the complement of MCP's installed, and data are being collected. A brief progress report is included as Appendix II.

#### VI. TASK 4 ACTUATOR MECHANISMS

All work on the mechanical assemblies is now completed except for environmental testing.

## VII. TASK 5 FILTER DEVELOPMENT

We have now concluded our study of alternative filter materials. We have found that the titanium/antimony filter is exceptionally good, providing a new EUV bandpass from 400 to 520 Å. Also, the material seems extremely stable against environmental degradation, making handling of the filter an easy task. The sensitivity of the filter is also quite good, since its transmission occurs between the bright 304 Å and 584 Å airglow lines. As shown in figure 8 of Appendix III the Ti/Sb/Ti filter is a full factor of five more sensitive than the other filters in the 200-900 Å region. Full details are given in Appendix III, which completes the filter development study.

## VII. TASK 6 PROCESSING ELECTRONICS

Breadboards of the electronic circuits have been individually checked out and they operate satisfactorily in most cases. The amplifiers, though, are being redesigned in order to handle the large capacitance of the wedge and strip anode with no adverse effect on the gain. Another circuit undergoing some degree of revision is the PPA. A critical component of the PPA is a DAC, and the current design includes an 8-bit DAC with 1/4 LSB accuracy. This allows the 256 x 256 pixel image plane to have pixels whose are can vary by as much as  $\pm 50\%$ , theoretically. (In practice, much better results are generally obtained). In order to avoid this circumstance, we are looking at incorporating a 12-bit, 1/2 LSB DAC into the circuit, which should give pixels with better than  $\pm 3\%$  uniformity. Additional progress includes the nearly complete wiring up of the electronic components not affected by the above mentioned changes, and a GSE for operating and testing out the complete electronics system has been completed.



## ATTACHMENTS

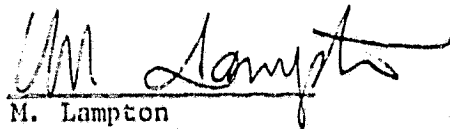
- Appendix I.            Technical Critique of JHU Preliminary Project Definition Document.
- Appendix II.          Interim Report on MCP Lifetest.
- Appendix III.        Final Report on Filter Development for the Extreme Ultraviolet Explorer
- Appendix IV.        EUVE Instrument Parameter Update.

APPENDIX I

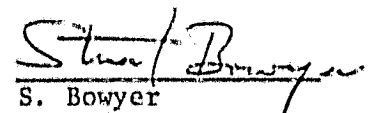
Technical Critique of the J.H.U.  
Preliminary Project Definition Document  
SCO/STO - 916

16 May 1980

Prepared by:

  
M. Lampton

Approved by:

  
S. Bowyer  
Principal Investigator

## 1. INTRODUCTION

This technical critique constitutes part of the U.C. Berkeley quarterly report for work accomplished under contract NAS 5-24445.

As part of Johns Hopkins University's Applied Physics Laboratory Study of the technical and operational feasibility of the Extreme Ultraviolet Explorer mission, a preliminary project definition document was prepared. That document, SCO/STO-916 (dated October 1978) has been made available to the UC Berkeley EUVE team for comment and updating. Some portions of the JHU study address management tasks specific to GSFC/JHU program procedures (e.g. sections 1,3.1,4.1,4.2) and will not be addressed in this report. Instead we shall cite those areas of the JHU document in which technical developments or engineering experience have introduced revised or refined estimates of the baseline EUVE mission requirements.

## 2. DOWNLINK REQUIREMENTS & IMPLEMENTATION

The JHU document baselines a scientific data rate accommodation of 3200 bps during darkness (see Sections 3.4,4.5,4.6, and Summary Table 1). This figure was adopted from an earlier (1976) document stipulating 50 photons per second (800 bps) per telescope as a minimum acceptable scientific return.

However, that figure was never intended to represent an optimized science throughput, and the EUVE Science Team has since conducted a study quantifying the dependence of scientific value (parameterized by survey sensitivity) upon telemetry data rate. The study shows that, under the background-photon-limited conditions encountered in EUV astronomy, the sensitivity increases with increased downlink data rate. Moreover, this sensitivity vs

(  
bit rate curve has a slope that depends on the particular waveband within the EUV. Consequently in a mission optimized for scientific return, the four telescopes would ideally occupy differing fractions of the data stream, rather than each being assigned a fixed 25% of the science. A companion report summarizing this study discusses these options and shows the desirability of providing a total nighttime science data rate considerably higher than the JHU figure.

Related to the downlink requirement is the complex subject of implementation. The JHU report identified three areas needing further study before a downlink system could be baselined. First, onboard data storage is required to span portions of the orbit for which both TDRS spacecraft are below the horizon; tradeoff between dual tape recorders versus bubble memories should be examined. Second, transponders having TDRS compatibility and an adequate power margin to handle the downlink traffic remain to be identified. Third, the perhaps most critical unknown revealed by the JHU report is the questions of which downlink antenna will best serve the EUVE mission. Their recommendation was a pair of biconical pattern antennas oriented along the plus and minus spin axes. Each of the four beams would have a gain of 7.7 dBi. However, if an active electronically steered antenna were otherwise compatible with the mission, such a device could offer substantially greater link margins and/or data rates. A re-examination of these options ought to be made a high priority item.

### 3. ATTITUDE CONTROL AND SPIN RATE

The JHU report baselines a continuously rotating spacecraft whose spin axis is kept within one or two degrees of the solar direction by the use of magnetic torque coils and an onboard sun sensor and control box (see JHU sections 3.5, 3.10, 4.8, 4.12, and Summary Table 1). This basic system layout appears to us to combine the advantages of autonomous attitude control with a simple and potentially reliable onboard control system.

However, the choice of spin rate is governed by the alternatives chosen in several hardware-dependent areas. JHU has recommended a spin rate of 0.1 rpm, a rather low value which we feel may have been forced by their adoption of the Ball Brothers CT-401 Star Camera as a precision attitude determination sensor. Other sensors are available which offer potentially lower initial cost, simpler interfacing, and lower continuing data analysis costs for attitude determination, while providing adequate attitude accuracy. One example is the Ball Brothers CS-201 Star Scanner. Its use may allow or require a somewhat higher spacecraft rotation rate. A higher rotation rate may, in turn, eliminate the need for an onboard momentum wheel. Other sensors probably exist. It is important to examine the range of candidate star sensors prior to adopting a nominal rotation rate.

A second constraint on the spin rate is the scanning blur accompanying the detection and telemetry of EUV photons with finite timing bins. This constraint takes the form of an upper limit on spin rate which is proportional to the bit rate of the slowest-telemetered scanning telescope. Since the overall spatial resolution target is 6 arc minutes ( $0.1^\circ$ ) for the EUVE mission,

it seems reasonable to budget about 3 arc minutes for the rotational blur term. At one rpm, three arc minutes corresponds to a minimum of 1920 bits per second per scanning telescope.

A third potential constraint on the spin rate is applicable if no momentum wheel is used. The stability of the spin axis orientation is very important in the reduction of the aspect sensor data for reconstructing the astronomical survey. This stability is hindered by the gravity gradient torques but is improved by storing a large angular momentum. A spin rate of 1.5 RPM provides the same angular momentum as the Sperry/CTS wheel recommended in the JHU report (Section 4.8.3).

A fourth potential constraint on the spin rate is the impact of an active, electronically steered antenna, which may introduce a latency gap into the downlink data flow each time a beam reselection is necessary.

#### 4. RECOVERABILITY BY ORBITER

The JHU document assumes that there is a requirement that the EUVE spacecraft be recoverable from the Orbiter. Their baseline layout includes an RMS grapple fixture, and their propulsion system is sized to allow the EUVE to descend from its 550 km STS orbit.

In the UCB analyses of the mission profile, however, the probable benefits of recoverability are minor and the costs could be considerable. Three scenarios have been studied in which recoverability could be useful, but in none of these cases would the cost and STS time and safety impacts be easily

justified. A case one recovery might be beneficial immediately after release by the STS, if some EUVE failure were discovered that would compromise its mission. We would suggest that this kind of failure probability be minimized by prelaunch checkout preparations, and a possible brief checkout of critical EUVE systems when in orbit prior to release from the STS. The possibility of recovery shortly after release is complicated by the safety requirements to dump propellants prior to grappling. In the event of the failure of some critical EUVE system, safety considerations may not permit recovery.

A case two recovery would be useful if some EUVE failure occurred after ascent to the 550 km orbit. However, the recovery costs in this case are considerably greater because the EUVE must now perform a descent to STS altitudes, and the Orbiter crew must become involved with a rendezvous which could be rather time consuming.

A case three recovery might be envisioned at the end of the nominal one year EUVE requirement. There is no science requirement for post-mission hardware recovery.

If the EUVE is to be recoverable, the attitude control system would be impacted. In particular, there would be a possible need for a reaction wheel on board the EUVE. It is likely that EUVE could be grappled only if it is nonrotating. For stability in the presence of gravity gradient torques a momentum wheel may be essential.

## 5. TELESCOPE AND DETECTOR ADVANCES

Although the JHU report did not specifically deal with details of the scientific experiment package, we note here that continuing research in the areas of optics design, EUV filter technology, and detector technology have made some of the instrument descriptions obsolete. An update on these areas has been prepared separately (see EUV Explorer Instrument Description, UCB SSL draft of 15 May 1980).

## 6. CONCLUSION

We have reviewed the recommendations of the JHU Applied Physics Laboratory and found several topics needing further examination. The areas which need additional near-term study in firming up the EUVE mission profile are the downlink implementation and the spin rate/ACS tradeoffs. The results of decisions taken in these two areas will have important consequences for the other aspects of the mission plan.

We recommend that EUVE not be recoverable from the STS as we do not believe the added benefits warrant the cost involved.



APPENDIX II

Interim Report on MCP Lifetest

16 May 1980

Prepared by:

Douglas R Rogers  
Doug Rogers

Approved by:

Stuart Bowyer  
Stuart Bowyer  
Principal Investigator

### 1) Lifetest Facility:

Lifetest tank has been pumped down since 4/22/80 with eight pairs of plates installed and connected to HV and monitoring electronics. Within one week after pumping down it was noticed that the Hamamatsu and Amperex plates had background rates of several hundred per second. The Hamamatsu plates were disconnected from the HV on 5/12/80 because it was determined that they were the cause of the high background rates on all other plates. Thirteen hours after the Hamamatsu's were disconnected a pair of Galileo plates suddenly became very active and this resulted in increased count rates in its two closest neighbors. On 5/14/80 the Galileo plates were causing so much noise in the other plates it was necessary to disconnect them from the HV.

Today there are six pairs of plates running: Amperex, Litton, ITT, Varian, a chevron pair from Galileo and a saturable plate from Galileo. All have relatively low (<30 cps.) backgrounds, except the Amperex, which sometimes climbs to over 100 c.p.s. The disconnected Hamamatsu and Galileo have been briefly reconnected at times and the result is an immediate climb in the count rates for all plates. Pressure in the lower half of the tank is  $\sim 4 \times 10^{-7}$  Torr, pressure in the upper half is  $\sim 7 \times 10^{-6}$  Torr. The tank will be brought up to air within a few days for leak testing, addition of newly calibrated plates and modifications such as shielding and repositioning of plates.

#### Problems:

1. Why does a noisy plate cause increased counts in other plates? (Also the image from a noisy plate is noticeably affected by which neighboring plates are connected to the HV).
  - electronic crosstalk? (this has been checked)
  - ion production by noisy plate?
  - increased outgassing by active plate?
  - electric fields?
2. How can the plates be isolated from one another?
  - simple electrostatic shielding around each holder?
  - (this will be tried)
  - major revision of lifetest tank
3. Why are some plates becoming so noisy?

4. Why is there still such a large pressure difference between the top and bottom of the tank? (it will be leak checked)
5. How can the pressure in the top half of the tank be monitored continuously without flooding the plates with ions?

## 2) Gerry's Tank

This tank can be pumped down from atmospheric pressure to a pressure for operating MCP's in about 15 minutes, so it is ideal for trying quick experiments. Experiments can be done on the pair of Nitech plates which Jay Freeman fried in his corona experiments and on a pair (Varian?) which has been sitting in the N<sub>2</sub> cabinet which has one broken plate.

Some of the things to investigate are:

- ion feedback
- corona discharge
- effect of old hot spots
  - dust
  - cleaning with alcohol
  - fingerprints
  - moisture
  - hairs and lint
  - baking out under vacuum
  - baking out at atm. pressure
  - cleaning with LN<sub>2</sub>
  - reverse voltage
  - short circuits between shims
  - running broken plates
  - running two sets of plates and moving them close to and away from each other
  - how hard it is to break a piece of the broken plate
    - by dropping, cracking, crushing, scratching, chipping,
    - thermal expansion, etc.
  - other ideas?

## 3) Plates still to be calibrated

These include one pair from ITT, Amperex, Hamamatsu, Nitech, another pair from Nitech and a saturable plate from Galileo. There is also the fried Nitech pair and the broken (Varian?) pair. Chris and Pat have run a Nitech pair and the ITT pair and had bad problems with both. Calibration of these plates should begin Friday or Tuesday.

APPENDIX III

Final Report on Filter Development  
For  
The Extreme Ultraviolet Explorer

9 May 1980

Prepared by:

1. Kimble  
Randy Kimble

Patrick Jelinsky  
Patrick Jelinsky

Approved by:

Stuart Bowyer  
Stuart Bowyer  
Principal Investigator

## SUMMARY

We report below on the results of the filter development contract NAS5-24189 for the Extreme Ultraviolet Explorer (EUVE). The purposes of the study were to identify, develop, and evaluate thin film filters with EUV bandpasses unattainable with previously available filter materials.

In the early stages of the study, titanium and antimony were identified as the most promising materials for providing the scientifically important 350-500 Å bandpass heretofore unattainable with thin film filters. A subcontract was let to the Luxel Corporation, who succeeded, after overcoming a number of technical problems, in fabricating pure titanium foils and titanium-antimony sandwich foils of the required uniformity and durability. Transmission measurements and optimization studies performed at Berkeley indicate that the titanium-antimony combination provides an ideal bandpass for scientifically valuable, high-sensitivity observations with EUVE. Environmental testing of the mechanical strength, moisture sensitivity and aging characteristics of the newly developed filter materials demonstrate completely flightworthy performance. The titanium-antimony filter will be a valuable addition to the EUVE filter complement.

## I. INTRODUCTION

Bandpass filters are essential to EUVE because of the sensitivity of the EUV detectors (microchannel plates) to far UV radiation (1000-3000 Å), a band in which the sky and most point sources are much brighter than in the EUV, and to charged particles. In addition, filter materials and thicknesses can be selected to minimize the background from the strong geocoronal and interplanetary EUV lines such as HeI 584 Å and HeII 304 Å, whose diffuse emissions would otherwise seriously impair the sensitivity of a photometric measurement. Furthermore, broadband EUV filters can perform the same scientific function as optical photometric filters, that of providing basic information about the temperature and chemical composition of a source, while maintaining high sensitivity.

EUV radiation does not pass through any thick crystal or stretched plastic sheets such as used in the far UV or soft X-ray respectively. The filter materials used in the EUV must be only a few thousand Å thick to be sufficiently transmitting for use on EUVE. Fortunately, vacuum deposition techniques have been developed over the years to allow the fabrication of large area, durable filters of metal and plastic as thin as 1000 Å or even less.

The baselined filter complement for EUVE was drawn from the commercially available and space-qualified materials used in various solar, atmospheric, and celestial experiments prior to the original EUVE proposal. That filter complement included:

1. Parylene. Parylene N is a plastic material which can be vacuum

deposited like a metal to form a filter as thin as 1000 Å. This provides a bandpass from 44-300 Å which is excellent in the study of sources in the transition region between the soft X-rays in the EUV. This is the EUV bandpass with the largest visibility through the interstellar medium. The turnon wavelength of the parylene - filtered telescope is determined by the design of the grazing incidence optics. The long wavelength cutoff is set by the thickness of the filter itself, selected for optimum sensitivity.

2. Aluminum. Aluminum has been the workhorse of EUV astronomy. It is sensitive from 180 to 600 Å, yet is opaque to the far ultraviolet. When used in combination with a thin layer of carbon to reduce the throughput of the bright 304 Å background line, it yields a 180-350 Å bandpass, making it the most important filter for purely EUV astronomy.

3. Tin. Tin has an excellent window from 500-750 Å. Its biggest drawback is the presence of the bandpass of the strong interplanetary 584 Å line.

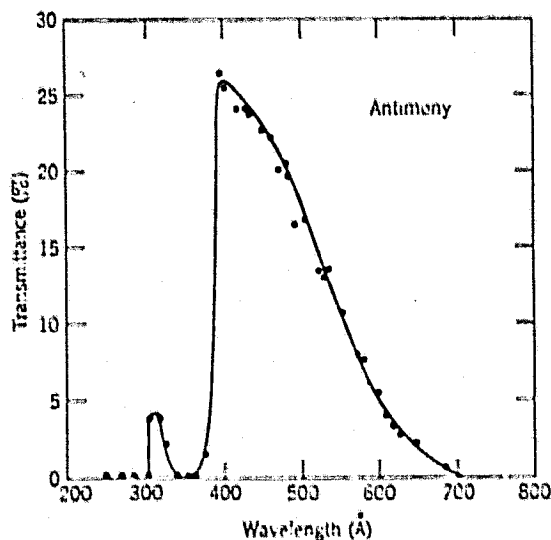
4. Indium. Indium has a window reaching from 750 to greater than 1000 Å. If made sufficiently thick, its grasp can be restricted to lie below the 912 Å Lyman edge, making it a truly EUV filter. The strong absorption of the interstellar medium near the Lyman edge restricts observations through this filter to only the nearest stars.

The most striking failing of the filter complement described above is the lack of a filter to cover the 350-500 Å band, between the bright 304 Å and 584 Å background lines. This central region of the EUV has

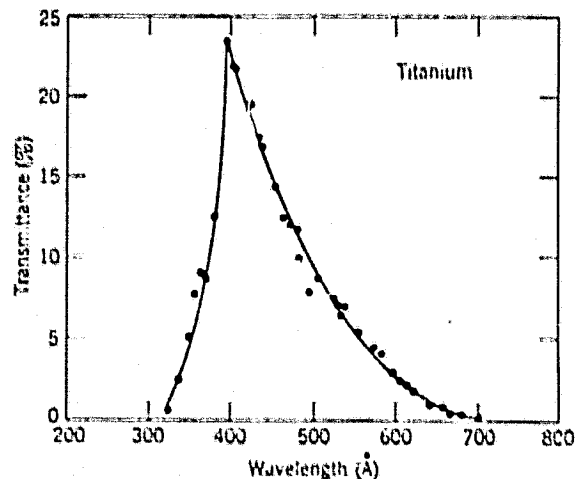
great scientific potential. It lies at wavelengths sufficiently removed from the Lyman edge that visibility is still reasonably good through the ISM. However, this bandpass is the range in which the EUV flux from a number of sources such as hot white dwarfs will be turned over by interstellar absorption, so it can provide important information about the local ISM. In addition, the exclusion of the strong background lines from the bandpass allows great increases in sensitivity to be attained. For these reasons, the EUVE filter development study concentrated on materials with potentially useful bandpasses in the 350-500 Å range.

## II. SELECTION AND FABRICATION OF NEW MATERIALS

The most promising materials for covering the 350-500 Å bandpass were identified through a search of the literature on the transmission properties of thin foils and through discussion with experts in the fabrication of such foils. The best compilation of transmission data is given in Samson's Techniques of Vacuum Ultraviolet Spectroscopy. The materials selected for fabrication after these investigations were antimony and titanium. The transmission properties of these materials as compiled by Samson are shown in Figure 1.



Transmittance of antimony 1000 ± 100 Å thick



-4- Transmittance of titanium 525 ± 50 Å thick



The existence of transmission data such as this showing appropriate passbands does not guarantee the suitability of the material for the EUVE application for several reasons. First, the transmission characteristics are typically well known only in the peak transmission range of the material. The sensitivity of the EUVE detectors to a wide range of wavelengths makes it essential that there be no secondary window in addition to the basic astronomy window. Even residual transmission in the wings as low as  $10^{-6}$  can be unsatisfactory because of the existence of the extremely strong hydrogen Lyman  $\alpha$  1216 Å diffuse background line. Hence a thorough investigation of the entire detector sensitivity range is essential for qualification of an EUVE filter.

Second, the transmission data for such materials are traditionally determined from extremely small foils and measured immediately after their fabrication. Hence it was never previously determined whether uniform, mechanically durable foils of sufficient size could be fabricated from these materials. Furthermore, no data existed on the longterm stability of the thin foils, which are in general susceptible to pinholing due to ambient moisture and to slow transmission decays with time from a variety of causes even in the absence of moisture (increasing oxidation of the surface, formation of intermetallic compounds in sandwich foils, etc.).

Hence, it was the purpose of this study to successfully fabricate large foils, verify the suitability of the overall transmission characteristics, and verify the mechanical and longterm transmission stability essential for space application.

### Fabrication

The fabrication efforts were subcontracted to the Luxel Corporation, whose president, Gordon Steele, has performed pioneering research in the fabrication of thin film filters. We review here the fabrication efforts that led to the final result of the filter study, a titanium-antimony combination foil which is strong, stable, and well-suited to high sensitivity observations with EUVE.

There are three conventionally used techniques in the deposition of metal films: evaporation from a tungsten filament, evaporation from a heated crucible, and electron bombardment. The fabrication difficulties presented by antimony required experimentation with all three techniques before a successful approach was found.

The tungsten filament deposition technique relies on wetting of the tungsten filament with the metal to be deposited. The metal evaporates from the hottest part of the filament while new metal is drawn to the evaporation point by capillary action. The properties of antimony render it unsuitable for this technique. The evaporation temperature of antimony is sufficiently close to its melting point that as soon as the metal is heated enough to flow, it flash evaporates, stopping the wicking action and preventing smooth deposition. It is sometimes possible to overcome this type of problem by alloying the unsatisfactory material with small percentages of another metal. Such alloying agents must not only be chemically suitable, i.e. must not form intermetallic compounds, but must not disturb the valence electron density so as to preserve the bandpass transmission. It was hoped that germanium would permit smooth

deposition when alloyed with antimony, but such attempts were unsuccessful.

With the heated crucible technique, it is possible to produce a more constant deposition rate, and antimony foils can be produced by this process. However, pure antimony foils reveal two major problems. They are found to be extremely moisture sensitive, developing pinholes if there is any residual moisture in the organic solvent used to release the deposited foil from the ceramic substrate. Second, even foils successfully released from the substrate are found to be extremely non-uniform. The antimony atoms move along the surface of the ceramic substrate until nucleation centers form, leading to unacceptable irregularities in thickness and transmission.

Deposition by electron beam bombardment permits all of the above problems to be overcome. This technique is essential for the deposition of titanium, whose melting point is too high for the filament or crucible techniques. The electron beam technique permits deposition of uniform titanium foils, which are interesting in their own right for EUV astronomy applications, and which provide the solution to the antimony fabrication problems. Thin titanium films perform as an active nucleating surface and a protective overcoat layer when deposited before and after an antimony layer in rapid sequence in a single vacuum. Whereas 1500 Å thick pure antimony films exhibit a mottled transmission in the red, evidencing the non-uniformity, the same thickness deposited between two 100 Å thick films of titanium is uniformly opaque and demonstrates a low susceptibility to pinhole formation during processing.

These experimental considerations led to the eventual selection of

films fabricated by Luxel and delivered to the Space Sciences Laboratory for testing and qualification: pure titanium filters of 500 Å and 1000 Å thickness, and titanium-antimony sandwich filters of 1100 Å antimony between 100 Å layers of titanium.

### III. TRANSMISSION MEASUREMENTS

Transmission measurements of the Luxel filters were carried out in the EUV calibration facility here at the Space Sciences Laboratory. The data which must be determined are the absorption coefficients of pure antimony and titanium and the transmission characteristics of any oxide layer that forms on the foils. This data is necessary for determination of the optimum filter design for EUVE, given the optics design, detector performance, and available telemetry. The optimization procedure, which determines the filter thickness with highest sensitivity and greatest scientific return, is described in a later section. No pure antimony foils were made (for the fabrication reasons described in the last section). Nevertheless, the necessary separation of absorption coefficients can be made by measuring the transmissions of titanium films of different thicknesses and of the sandwich film, which provides enough independent data to solve for the three unknowns.

The transmission measurements were performed using a grazing incidence monochromator to select line radiation from a hollow cathode discharge source. The detector used was a calibrated one inch diameter channel electron multiplier (channeltron). The dynamic range of the detector was extended using calibrated meshes to attenuate the direct monochromator beam. All measured count rates were corrected for electronics deadtime, and off-line

background measurements permitted the subtraction of spurious counts due to scattering in the monochromator.

Transmissions were measured at wavelengths from 130 Å to 2300 Å. For some wavelengths far into the wings of the filter bandpass, only upper limits could be found to the transmission. These upper limits are sufficiently low that the sensitivity of EUVE using the optimum thickness filter of these materials is independent of the actual value of the transmission for these far-off bandpass wavelengths.

The transmission curves for the two titanium thicknesses and titanium-antimony sandwich are shown in Figures 2-4. This is the raw data except for removal of the 80% transmission factor of the nickel support mesh on which the films are mounted. These transmission curves show several interesting features. The titanium transmissions confirm the existence of a second transmission window from 250 Å to X-ray wavelengths not shown by Samson, but reported by Sonntag et al. (Solid State Communications 7, 597, 1969). The overall behavior appears to be that of a broad transmission window beginning at  $\sim 700$  Å and containing a strong absorption line at  $\sim 300$  Å.

The predominantly antimony filter also showed the same overall transmission behavior as in previous studies. However, when actual antimony transmission was separated out, it was found that the pure antimony transmission was a factor of three higher than previously published results (Rustgi, JOSA 55, 630, 1965). We obtained a maximum of 85% transmission for an 1100 Å thick antimony foil, whereas Rustgi reported 25% maximum transmission for the same thickness.

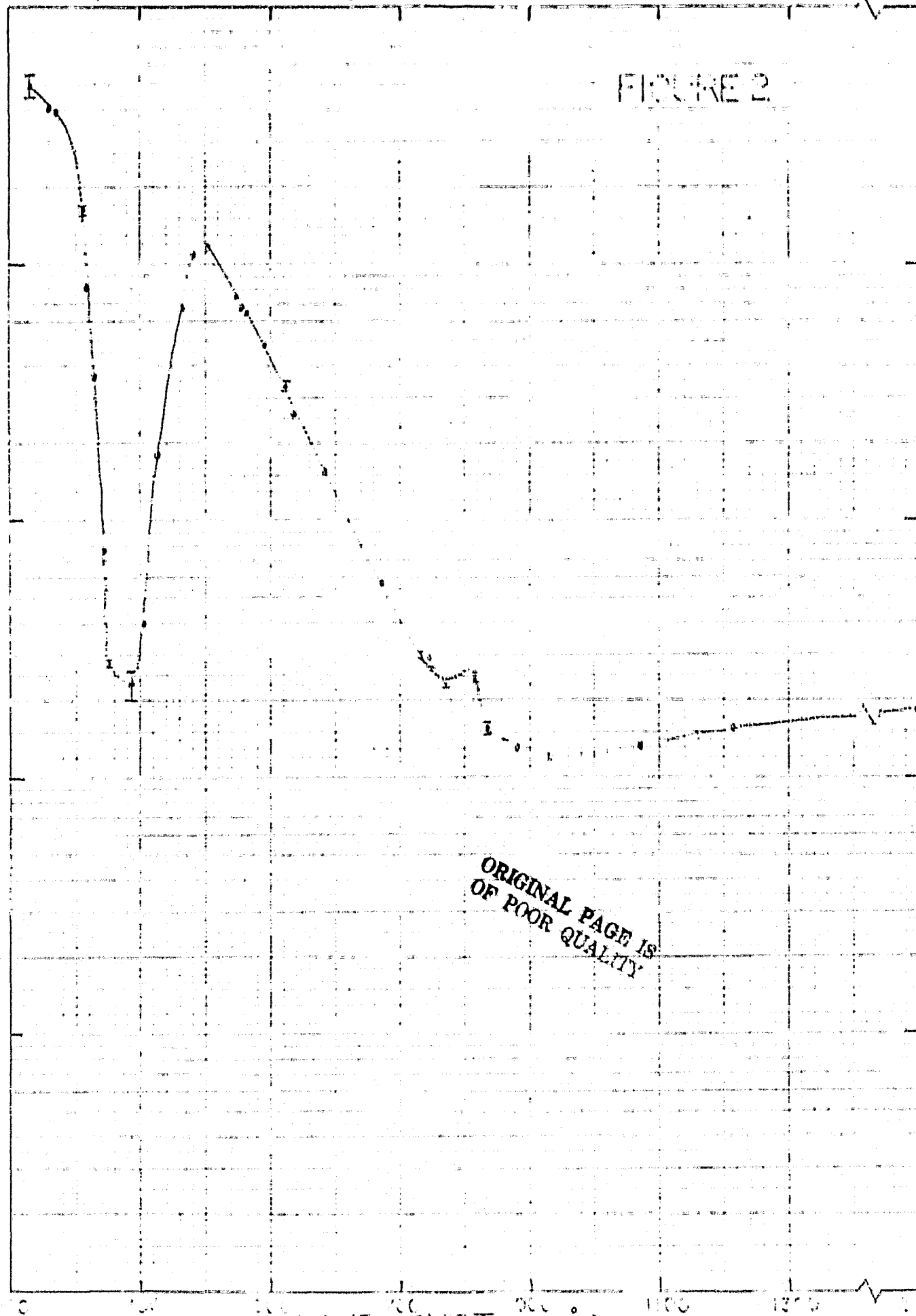
Examination of the Rustgi reference revealed that the antimony foil

# TRANSMISSION OF TITANIUM VACUUM TUBE

FIGURE 2

46 6210

SEMI-LOGARITHMIC 5 CYCLES X 7.5 DIVISIONS  
JAN 61 PEGFEL & ESSER CO. M01 0014



ORIGINAL PAGE IS  
OF POOR QUALITY

# TRANSMISSION OF TITANIUM DIOXIDE

FIGURE 3

46 6210

MEAN OF 10 OBSERVATIONS X 10<sup>4</sup> D. 10.005  
DETERMINED BY 10.005

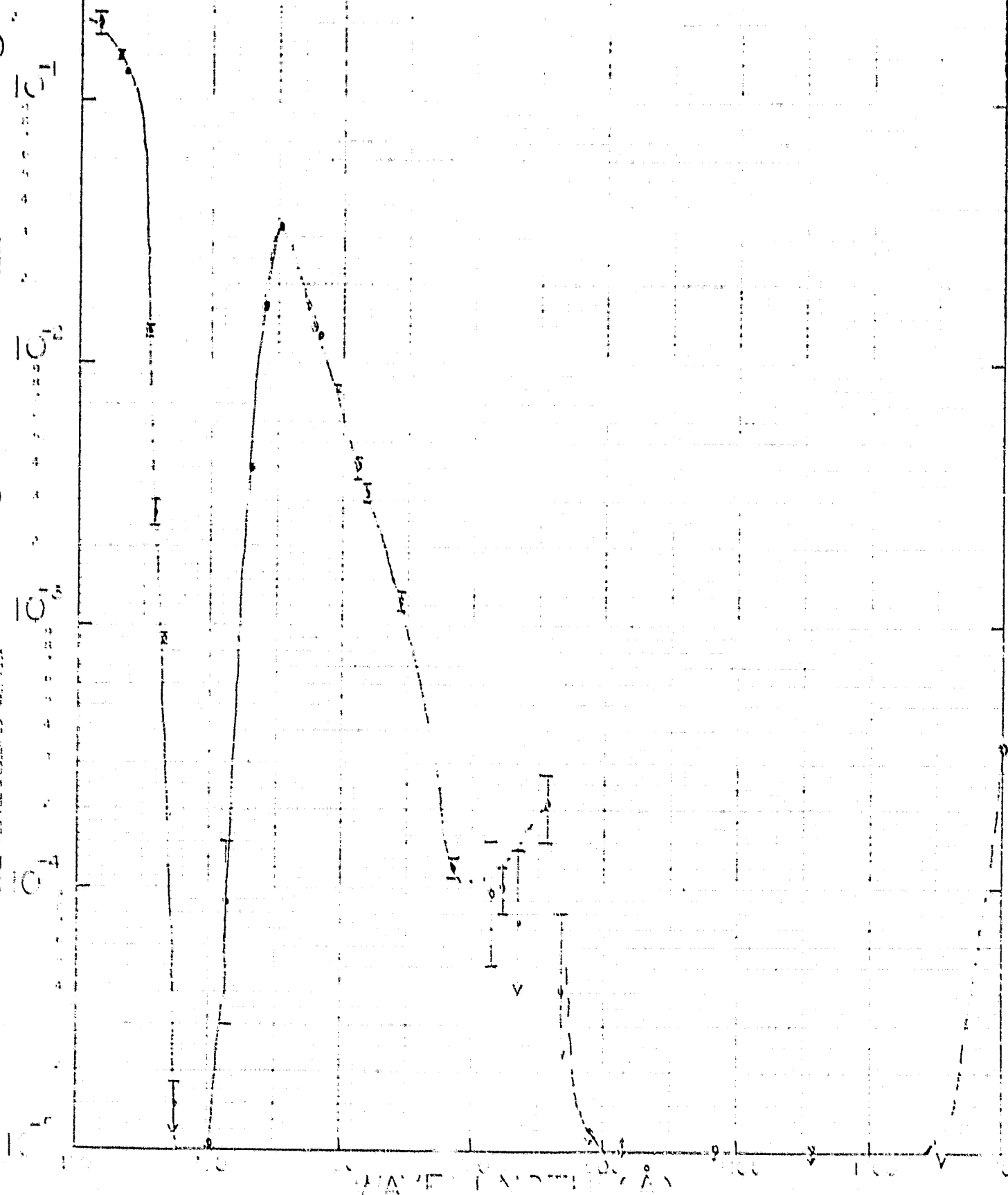
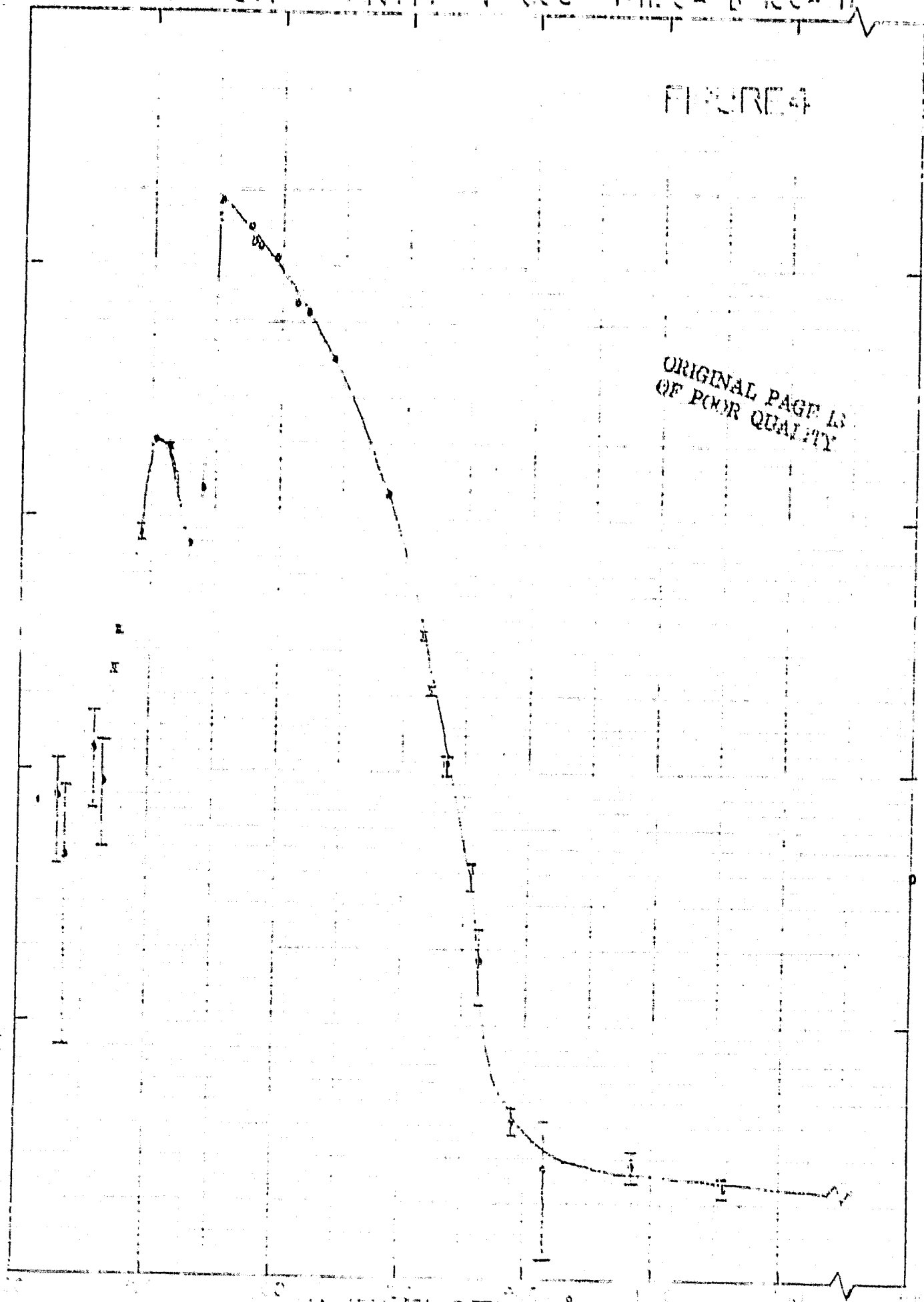


FIGURE 4



ORIGINAL PAGE IS  
OF POOR QUALITY

46 6210

NOTE: REMAINING DATA OF COMPLEXES / REDUCED  
PRESSURE / REDUCED PRESSURE



used for that measurement had been deposited on aluminum, and then the composite foil was floated off the substrate in water. This cannot have given a valid measurement, since the intermetallic compound aluminum antimonide would have formed at the interface and the outer layer of the antimony would have been heavily oxidized by the direct exposure to water. The foils produced by Luxel however, are Ti/Sb/Ti sandwiches in which all three layers are vacuum deposited at the same time, removed from the substrate in an organic solvent, and kept in a dry atmosphere thereafter. Thus there is no intermetallic compound formed, nor any antimony oxide. Our measurements should therefore give the true absorption coefficient for antimony.

The separation of the absorption coefficients is performed using the following relationships:

$$T(500) = \exp[(\mu_{Ti} - \mu_{TiO})x_{TiO}] \exp[-\mu_{Ti}(.05)]$$

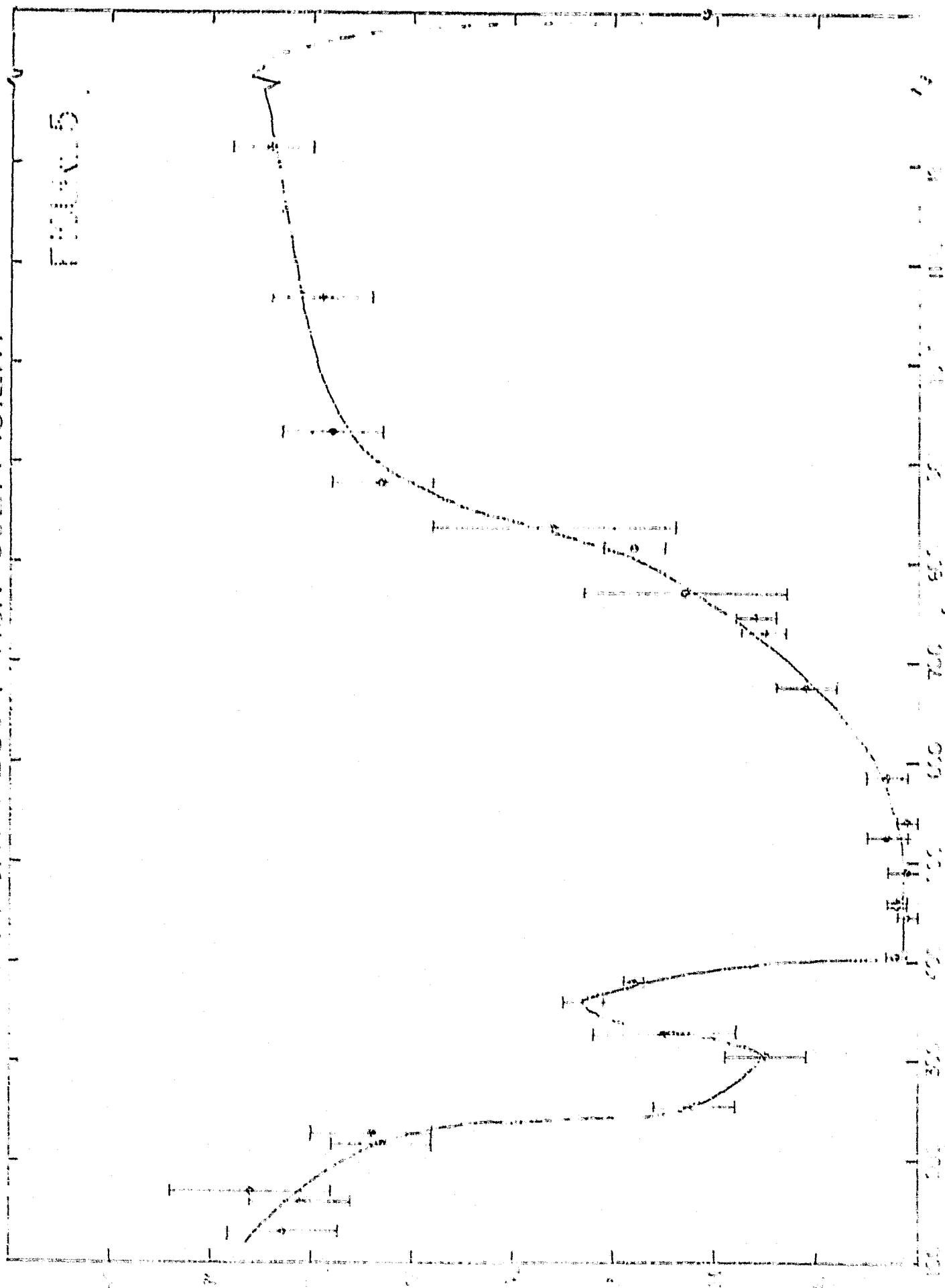
$$T(1080) = \exp[(\mu_{Ti} - \mu_{TiO})x_{TiO}] \exp[-\mu_{Ti}(.108)]$$

$$T(Sb) = \exp[(\mu_{Ti} - \mu_{TiO})x_{TiO}] \exp[-\mu_{Ti}(.020)] \exp[-\mu_{Sb}(.112)]$$

$T(500)$  and  $T(1080)$  are the transmissions of the 500 and 1080 Å thick titanium foils,  $T(Sb)$  is the transmission of the sandwich foil,  $x_{TiO}$  is the thickness of the oxide layer formed, and  $\mu_{Ti}$ ,  $\mu_{Sb}$ ,  $\mu_{TiO}$  are the absorption coefficients of titanium, antimony, and the oxide layer, measured in microns<sup>-1</sup>. One can solve for  $\mu_{Ti}$ ,  $\mu_{Sb}$ , and  $\exp[(\mu_{Ti} - \mu_{TiO})x_{TiO}]$ , yielding the absorption data necessary to predict the transmissions of filters of different thickness and hence optimize the EDVE design. The derived coefficients are shown in Figures 5-7.

# ANTIALNY ABSORPTION COEFFICIENT

Fig. 5



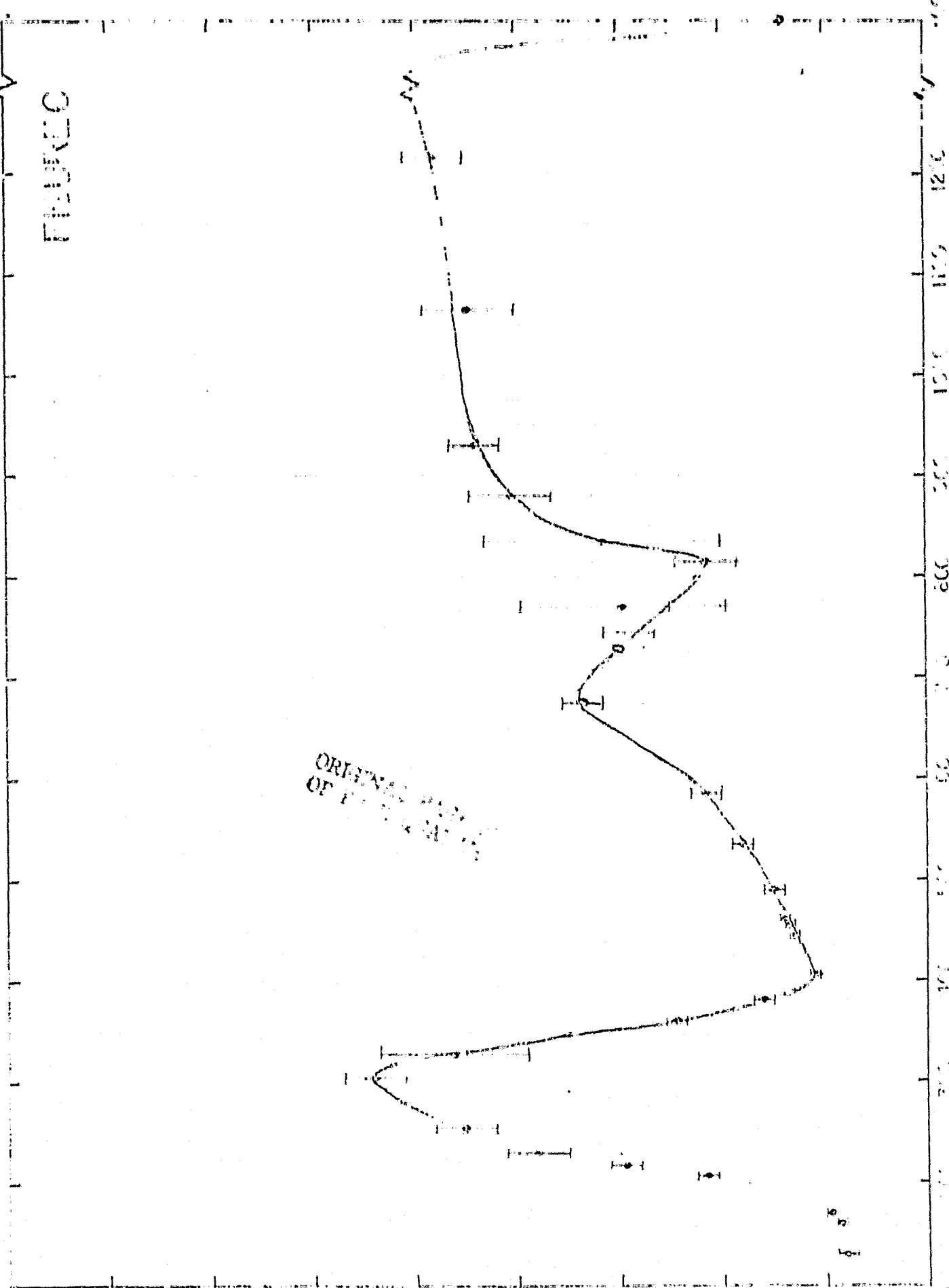
WAVELENGTH (nm)

TOTAL ABSORPTION COEFFICIENT

FIGURE

ORIGINAL DATA  
OF P. J. ...

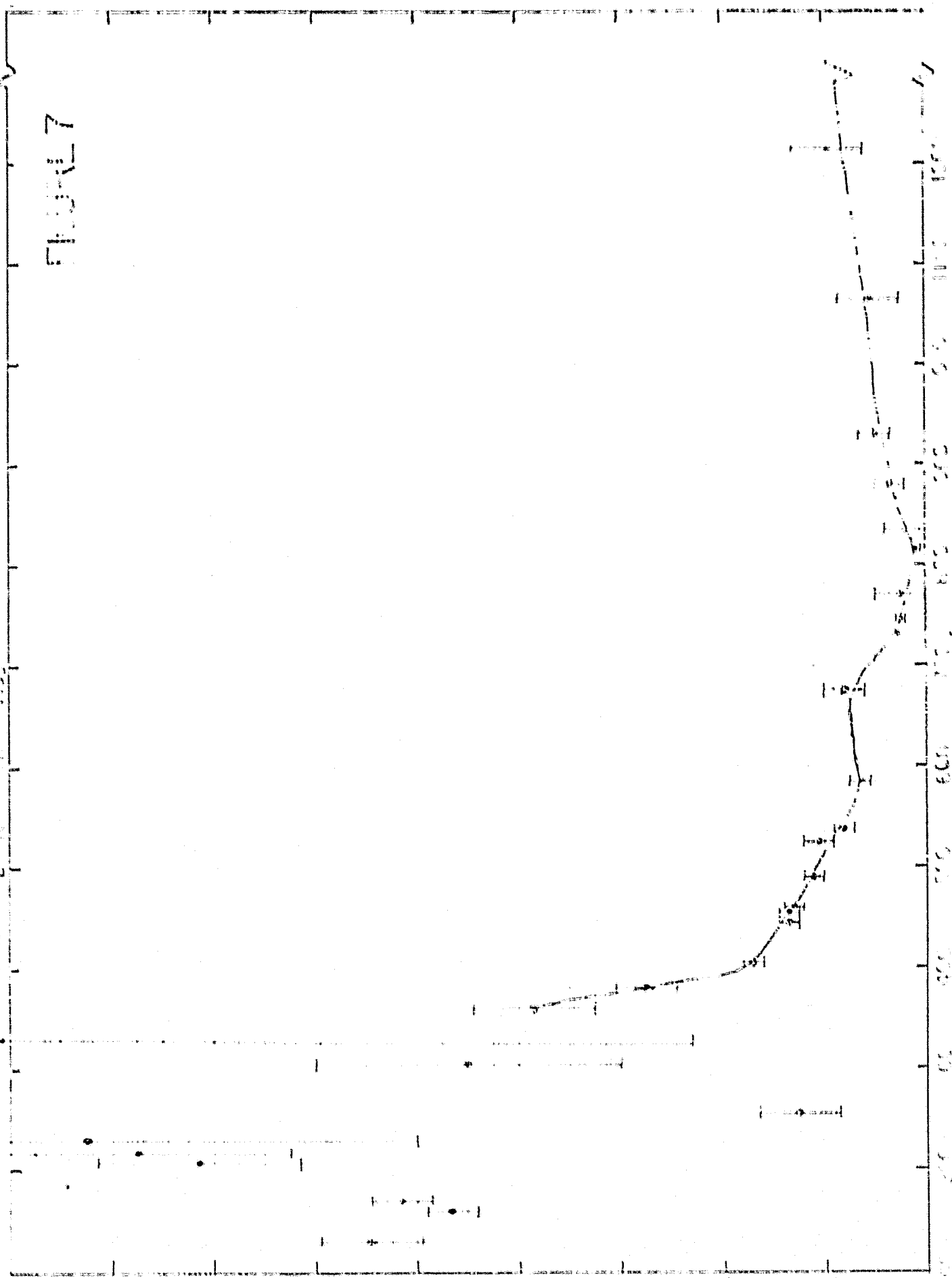
WAVELENGTH (Å)



$E/(E_0 - H_0)/X_0$

FIGURE 7

Wavelength (Å)



#### IV. SCIENTIFIC POTENTIAL ON EUVE

The achievable sensitivity of the EUVE using the newly developed filter materials has been determined using the filter optimization procedures developed for EUV astronomy here at the Space Sciences Laboratory. The overall sensitivity of EUVE of course depends on a wide range of instrument parameters: telescope size, field of view and angular resolution; detector quantum efficiency and spatial resolution; observation time and telemetry rate; filter transmission properties. All are subject to various constraints. Given a baselined instrument design, observing time, and telemetry capability, filter optimization consists of determining the filter thickness which yields the smallest detectable flux. For a sandwich filter thicknesses of the two filter materials are varied independently in the search. The resulting minimum detectable flux defines the instrument sensitivity. We briefly summarize here the optimization procedure.

##### A. Theory of Filter Optimization

A source has been detected with 99.9% confidence if the number of counts due to the source (in the source pixel) is at least three times the square root of the average number of counts in adjacent (background) pixels. This requirement leads to an expression for the minimum detectable flux,  $F$ , in photons  $s^{-1} cm^{-2} \text{\AA}^{-1}$  assuming that the source spectrum is flat within the bandpass.

$$F = 3 \sqrt{\frac{\omega}{T}} \sqrt{\frac{R_o f^2 + A \int t(\lambda) B(\lambda) d\lambda}{[A \int t(\lambda) d\lambda] (1 - e^{-tm/R})^2}} \quad (1)$$

where

$T$  = total observing time

$\omega$  = solid angle observed by one pixel

$A$  = effective area of telescope  $\times$  quantum efficiency (QE) of detector (assumed to be constant throughout bandpass)

$t(\lambda)$  = filter transmission at wavelength  $\lambda$

$B(\lambda)$  = background flux density at  $\lambda$

$R_D$  = detector background per unit area  $s^{-1} cm^{-2}$

$f$  = telescope focal length

$t_m$  = telemetry limit (cts  $s^{-1}$ )

$R$  = total count rate of detector (cts  $s^{-1}$ )

The computer routine utilized to optimize the filters for EUVE incorporates all of the data necessary for evaluating the minimum detectable flux  $F$ . It calculates an instrument throughput for every  $10 \text{ \AA}$  interval, accounting for variations in telescope response, detector quantum efficiency, and filter transmission with wavelength. It includes all known sources of diffuse radiation background from 10-2000  $\text{\AA}$ , as well as theoretical estimates in poorly measured regions of the spectrum. It calculates the minimum detectable flux for a given filter thickness or pair of thicknesses. In addition, it computes the mean wavelength, the total grasp and the grasp shortward of a chosen wavelength, which permits a determination of the approximate bandpass of the filter. (Grasp is defined as  $\int t(\lambda) d\lambda$ .)

The computation of the mean wavelength and grasp below a specified wavelength allows additional scientific judgment to be applied to the filter optimization. It is not necessarily true, for example, that the optimum

design of a sandwich foil is that combination of thicknesses which yields the lowest minimum detectable flux. Maximum scientific return from EUVE requires that bandpasses of the various filters remain distinct. Hence while an aluminum/carbon achieves the maximum sensitivity as the aluminum thickness goes to zero, such a design would not be chosen since the resulting bandpass would be identical to parylene. Hence an external constraint on the bandpass properties is sometimes imposed on the filter design and optimization takes place within that constraint.

#### B. Sensitivity results for titanium and antimony

Both titanium and antimony transmit well in the range from 400-500 Å. Optimum sensitivity results when the materials are used together. Pure titanium is inappropriate for covering the 400-500 Å bandpass because of the transmission window below 250 Å. Pure antimony can be improved by the addition of titanium because the titanium transmission falls rapidly above 500 Å, while that of antimony falls more slowly. Hence the addition of titanium attenuates the strong 584 Å background flux while preserving the primary bandpass.

The minimum detectable flux has been minimized with the requirement that less than 1% of the grasp lies shortward of 350 Å. Relaxing this requirement to 10% does not improve the sensitivity by more than 20%. With the 1% constraint the optimum combination is 1400 Å of titanium sandwiching 1000 Å of antimony. Such a combination presents no fabrication problems.

The resulting sensitivity of EUVE with the titanium/antimony sandwich filter and the previously qualified filters is shown in Figure 8. These sensitivities are derived assuming the baselined instrument parameters and

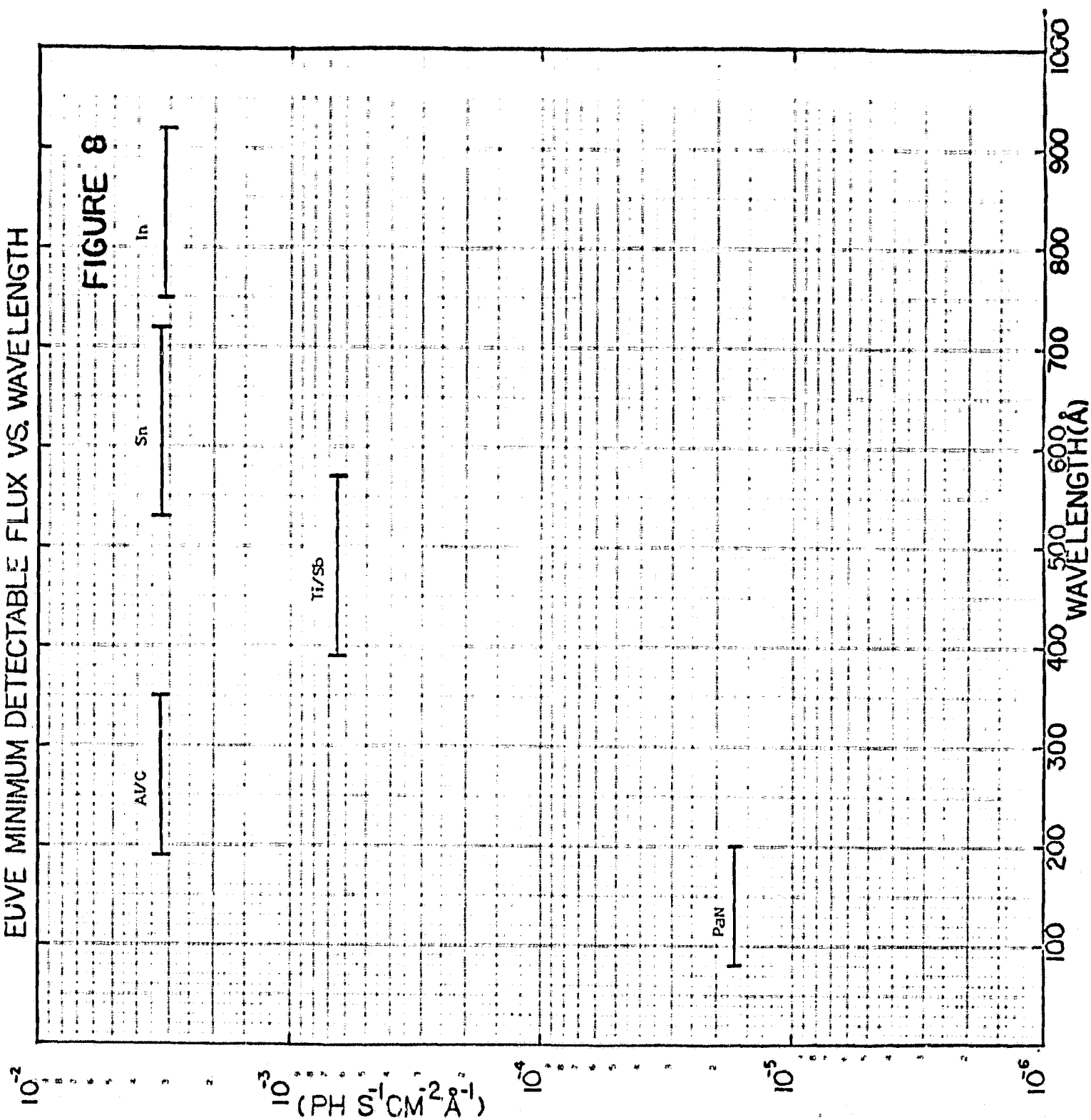
the baselined telemetry rate of 800 bits per second per telescope. The bandpasses shown are defined as the full width to 10% of maximum instrument throughput. A better representation of the spectral coverage of the filters now available is given by Figure 9, which presents the transmission curves for the optimized filter of each material or combination.

These figures dramatically illustrate the scientific potential of the newly developed filter combination. The titanium/antimony filter combination fills in the missing wavelength range in the baseline EUVE coverage and does so with a factor of five greater sensitivity than the other EUVE bandpasses.



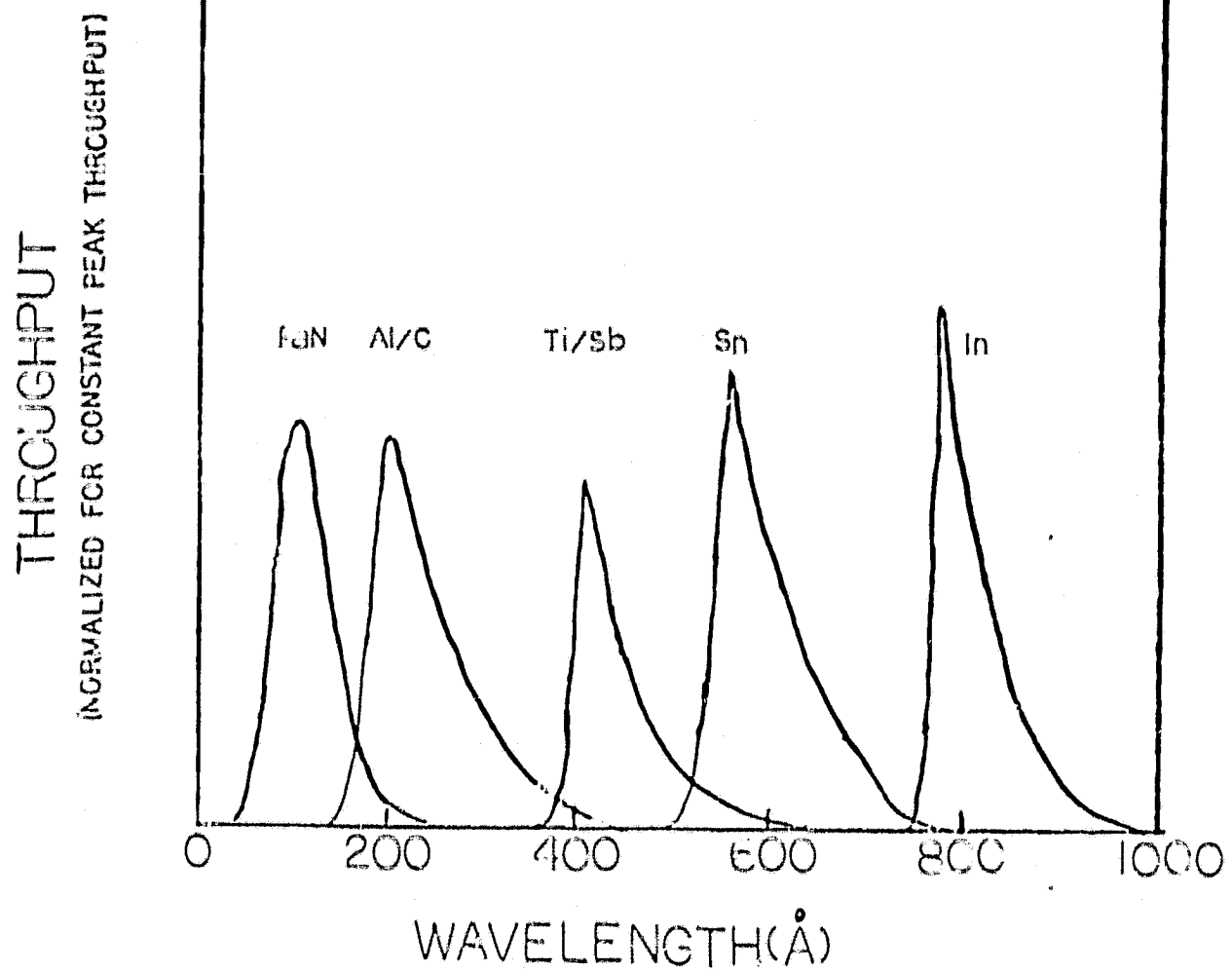
# EUVE MINIMUM DETECTABLE FLUX VS. WAVELENGTH

FIGURE 8



# EUVE BANDPASSES

FIGURE 9



## V. QUALIFICATION

The excellent transmission characteristics and potential EUVE sensitivities described in the previous sections are of course useless unless the titanium-antimony sandwich foil demonstrates acceptable longterm stability and mechanical strength sufficient for spaceflight qualification. The Ti/Sb/Ti filters have therefore been subjected to extensive testing of these characteristics. We describe here the tests of moisture-sensitivity, longterm transmission stability, and mechanical strength passed by the new filter.

### A. Moisture-Sensitivity

We present here excerpts from the report of the development subcontractor, Luxel, of the humidity testing of the titanium-antimony sandwich filter. This test is crucial to the qualification of a flight filter. Though the EUVE filters will be launched in vacuum, they will of necessity be exposed to the standard laboratory environment during testing and calibration unless extraordinary measures are taken.

"Aging Characteristics of Antimony Type XUV Filter Foil"  
Gordon Steele/Luxel Corporation

### Introduction

Submicron thick metal foils, employed as filters or windows for instruments functioning in the extreme ultraviolet and soft x-ray region of the spectrum, present special problems in common with their fabrication. Perhaps foremost among these is their proneness to develop 'pinholes'. Such pinhole defects may leak white radiation or may vacuum leak gas from a cell. The particular proneness of these foils toward this end is due their chemical reactivity in the presence of atmospheric moisture and their extremely thin nature. Many

metals which are noted for their durability in the earth's atmosphere in 'massive' form are unstable in submicron thick foil form. The reason for this is that the protective oxide layer formed on metals in their massive form usually exceeds the total thickness of submicron foils. Determining the durability and practicality of new materials, of interest for their special optical properties, is achieved by exposing the foil material to a standard degrading environment and measuring the visible light leakage as a function of time. Such is the subject of this report wherein the desired material is a metal foil of antimony and titanium.

### Discussion

Pinholes resulting from chemical action between a metal foil and the gaseous environment form with point attack such that a certain amount of time is required to penetrate the foil and thereafter the oxidation proceeds laterally in a 'burning grass' type of growth. Increased transmission with aging is due to enlargement of initial pinholes with very few new ones forming. Typically the initial stage shows very little pinhole transmission, but after this phase the transmission increases rapidly to some apparent plateau with a drift increase thereafter.

Two types of pinholes result from this action; virtual and real. Virtual pinholes, point leaks of visible light a few hundreds of nanometers in diameter, are determined by SEM to be oxidized metal structurally retained within the foil. Stoichiometric oxidation does not occur initially and thus visible transmission is primarily in the red. Subsequently, stresses developed through volume change in conversion to the oxide breaks the oxide out of the foil and a hole or real pinhole, a few thousands of nanometers in diameter, results.

Pinhole formation in submicron foils seems to occur at selected sites. It is believed that these are associated with a screw dislocation growth of the foil during formation. The principal factor contributing to pinholes is relative humidity. Trace amounts of acid forming gases such as carbon, sulphur and nitrogen oxide gases and particulates like salt have an accelerating effect in the presence of moisture, but none when dry. Therefore test aging of foils for pinholes development is done with an exposure to air adjusted to some constant relative humidity by a constant R.H. solution. Care must be exercised in selection of a R.H. solution since most of the handbook recommendations represent a particular concentration of salts which buffer the R.H. at some desired level. Our work finds that significant and variable amounts of acid gases exist in equilibrium with these solutions (i.e.,  $\text{CO}_2$  over  $\text{K}_2\text{CO}_3$  solution) which unreliably accelerates the results. Therefore this laboratory employs a 'clean' constant R.H. aqueous solution of sodium hydroxide recognizing that it not only adjusts the water vapor content but removes any acid gas traces that may be present in a laboratory environment (and also, one might add, the natural  $\text{CO}_2$  in air). Extensive testing has shown most submicron foil materials do not develop significant pinholes at less than 20% R.H. over an exposure of three months. At 60% R.H., chosen as a probable value for most field environments, the initial

or 'induction' stage for aluminum lasts about one week after which a three decade increase occurs. Indium and tin on the otherhand have induction phases of about three days with subsequent rapid deterioration over a four decade increase. Initial pinhole transmissions are generally about  $10^{-8}$  of incident light. After six weeks, pinhole transmissions are typically  $10^{-6}$  to  $10^{-5}$ .

#### Tests and Results

It was decided from experimental considerations that a filter comprised of 200Ti/1500Sb/200Ti foil would be optically suitable. Such a foil and filters thereof were fabricated and tested. Representative filters were stored in R.H. buffered closures at 60%, and -1% (desiccated) environments. From time to time, over a period of six weeks, the filters were removed for measurement of white light transmission in a PM photometer having a dynamic range of four decades. Initial transmission of each of the filters was  $4.0 \times 10^{-9}$  of incident light. The data, shown in Figure 1, demonstrates that the XUV foil material 200Ti/1500Sb/200Ti is very durable toward pinhole aging due to moisture. Over the period of the test no degradation was observed within the sensitivity range of the photometer ( $1 \times 10^{-9}$ ). For comparative purposes Figure 1 also includes the degradation which would be typical for a 1500Al:Si XUV foil similarly exposed to 60% R.H.

#### Conclusion:

1. Pure antimony foils are unsuitable as XUV filters from two practical points of view. First the evaporative techniques used to prepare submicron foils results in foils of mottled red transmission when 1500 Å thick. Second, pinhole-free antimony films are difficult to fabricate due to their high sensitivity to atmospheric moisture.
2. Providing 200 Å thick films of titanium as a nucleating surface and as an overcoat results in a sandwich foil of antimony 1500 Å thick which is very opaque to visible light and unusually resistant to pinhole formation when exposed to a 60% R.H. environment. This titanium-antimony laminant foil demonstrates aging characteristics which are superior to aluminum type XUV filters.

#### B. Transmission Stability

The transmissions of the filters were measured again one year after the initial measurements described above to ascertain the longterm stability of the titanium and sandwich filters. During that period the filters were exposed to the laboratory environment for a few weeks and stored in dry nitrogen for the rest of the time.

The results demonstrate remarkable stability, particularly for the



titanium-antimony combination. In the bandpass of the sandwich filter the transmission decreased by a maximum amount of 13%, while in the wings the transmission decreased by a maximum of 25%. The corresponding maximum decreases for the 1000 Å titanium filter are 12% in the bandpass and 70% in the wings. For the 500 Å titanium filter the results are 30% in the bandpass and 18% in the wings. Of particular interest is that at no wavelength did the wing transmission open up to indicate the development of pinholes. Rather the general behavior is for the ratio of bandpass to wing transmission to grow even higher.

This stability is excellent when compared with previously used EUV filters. Standard filters such as aluminum, tin, and indium show transmission drops in the bandpass of 20% in only three months. Hence it is conventional to procure flight filters as late as possible before launch or before they can be stored in vacuum. The titanium-antimony sandwich, with its superior longterm stability, therefore has no deleterious impact on the EUV filter storage requirements or delivery schedule.

#### C. Mechanical Strength

To determine the mechanical acceptability of the newly developed filter, the filters were vibration tested at NASA Ames Research Center. The filters tested had been mounted by Luxel in the standard manner they have developed for thin film filters. The foils are glued to an 80% transparent finely spaced nickel mesh glued around the edges to a rigid frame. Often for filters used in space research a bead of compliant epoxy is placed around the edge of the filter and filter frame. This procedure (called margining) greatly reduces the stress on the filter by distributing the loads at the interface to the frame.

The filters at launch are subjected to two types of stress, vibrational and acoustic. The extremely high strength-to-weight ratio of the foils and meshes enables them to withstand extremely high levels of vibrational loading. The acoustic stress tends to be much more severe. The EUVE filters will be launched in vacuum boxes with the detectors, eliminating the acoustic loading.

The vibration testing at Ames was performed with the 16 mm diameter filters used for the transmission measurements. These are probably smaller than the EUVE flight filters, which may be as large as 40-50 mm in diameter. However, the test was extremely conservative in two regards: the filters tested were not margined and the test was performed in air, rather than in a vacuum box. The large factor of increased stress from the presence of the acoustic loading more than compensates for the increased stress resulting from using larger filters. Hence we consider the test as a whole to be conservative with regard to the requirements of the EUVE flight filters.

Vibration testing was performed to the qualification levels of random vibration and sine sweep for the space shuttle. In addition, the filters were subjected a large amplitude sinusoidal vibration at a constant low frequency. This test has been used on some previous launch programs as a simulation of DC accelerations. Specifications for all three tests are given in Table 1.



TABLE 1

Random Vibration	(3 minutes, each axis)
20 Hz	.006 $g^2/Hz$
20-100 Hz	+6 db/octave
100-1000 Hz	.15 $g^2/Hz$
1000-2000 Hz	-6 db/octave
2000 Hz	.0375 $g^2/Hz$
14.7 grms overall	

## Sine Sweep (each axis)

1 g at 1.5 minutes/octave from 20-2000 Hz.

## DC Simulation (3 minutes, each axis)

20g at 50 Hz.

All filters tested (500 Å Ti, 1000 Å Ti, and the 100 Å Ti/1100 Å Sb/100 Å Ti sandwich) survived the random vibration and sine sweep with no damage.

The sandwich filter and the 1000 Å titanium filter survived the DC simulation with no damage. The 500 Å titanium filter developed pinholes during the DC simulation test. Hence, further testing under evacuated conditions would be necessary to qualify a filter this thin for launch. However, the 500 Å titanium filter is not useful for FIVE because of the large wing transmissions. The most important new filter developed, the titanium-antimony sandwich, shows excellent mechanical strength and will have no problem with FIVE launch.

## VI. CONCLUSIONS


1. Both pure titanium and titanium/antimony combination filters have been fabricated. The fabrication process is now well understood and filters of different thicknesses should present no problem.
2. The transmission properties of the two materials in combination and separately have been determined. With this data, the optimum filter design for EUV instruments using these materials can be determined.
3. The optimum titanium/antimony EUVE filter has been designed. With current design parameters and telemetry availability the optimum combination consists of  $700 \text{ \AA}$  Ti/ $1000 \text{ \AA}$  Sb/ $700 \text{ \AA}$  Ti. In combination with previously developed filters, the resulting sensitivity and spectral coverage offer dramatic improvement over the original EUVE design. The optimum EUVE filter complement now consists of parylene N, aluminum/carbon, titanium/antimony, tin and indium filters.
4. The titanium/antimony combination filter has undergone extensive testing of moisture sensitivity, longterm transmission stability, and mechanical strength. In all areas, the new filter demonstrates qualities equal to or superior to those of previously qualified EUV filters.
5. The new filter material has no impact on EUVE cost and schedule. Price and delivery of titanium/antimony filters will be similar to those of the other EUV filters.

APPENDIX IV

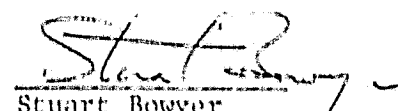
EUVE Instrument Parameter Update

15 May 1980

Prepared by:

  
Gerald Penegor

Approved by:

  
Stuart Bowyer  
Principal Investigator

# EUV EXPLORER INSTRUMENT

Preliminary Working Draft 5/15/80

## Description and Requirements for Shuttle Launch

### 1.0 Management Summary

1.1 Payload Title - Extreme Ultraviolet Explorer (EUVE)

1.2 Funding Agency - NASA

1.3 Key Personnel

Prof. Stuart Bowyer 415/642-1648

Dr. Roger Malina -2693

Dr. Frank Paresce -3524

Dr. Mike Lampton -3576

Mr. Hank Heetderks -5890

Space Sciences Laboratory  
University of California  
Berkeley, CA 94720

### 2.0 Payload Description

#### 2.1 Purpose

To conduct a sensitive astronomical survey of the entire celestial sphere at EUV wavelengths (70 to 900 Å).

#### 2.2 Technique

Four telescopes with detectors will be mounted on a spacecraft suitable for a Shuttle launch. The imaging grazing incidence optics with organic and metallic thin-film filters will be sensitive to selected bandpasses in the 70 to 900 Å region. One telescope will feed a gas proportional counter (PC) detector, the other three will feed micro-channel plate (MCP) detectors. Three telescopes will scan the sky at right angles to the spin axis, one telescope will point along the spin axis in the anti-solar direction.

## 2.3 Telescope Complement

All telescopes are Wolter-Schwarzschild Type 1

	<u>Scanner 1</u>	<u>Scanner 2</u>	<u>Scanner 3 *</u>	<u>Pointer 1</u>
Optical diameter	63.5cm	63.5cm	63.5cm	63.5cm
Flange diameter	76cm	76cm	76cm	76cm
Focal length	50cm	50cm	80cm	50cm
Geometric area	<del>180</del> cm <sup>2</sup>	<del>76</del> cm <sup>2</sup> 180cm <sup>2</sup>	100cm <sup>2</sup>	<del>76</del> cm <sup>2</sup> 180cm <sup>2</sup>
Field of view	3°	3°	3°	3°
Wavelength	600 Å	300 Å	200 Å	300 Å
Detector	MCP	MCP	PC/MCP	MCP
Overall length	100cm	100cm	160cm	100cm
Filters	2	2	1	compound

\* Design contingent upon Spacecraft compatibility. Optimum design listed here. Shorter overall lengths are possible to a minimum of 100 cm.

## 3.0 Launch and Orbit Characteristics

3.1 Launch Window - no restrictions

3.2 Orbit Parameters

550 ± 50 km, 28.°5 inclination

3.3 On-orbit life - One year

## 4.0 On-orbit Stabilization and Orientation

4.1 Look Direction - anti-solar for pointing telescope

perpendicular to sun line for scanning telescopes

4.2 Attitude Stabilization

Solar spin stabilized at 4 rpm max @ 8000 bps/telescope with optimum spin rate dependent on the telemetry allocation.

Spin axis controlled to ± 1° and knowledge to .05°

#### 4.3 Attitude Determination

Final determination of spin axis and telescope line of sight after all error contributions, should be  $\leq .1^\circ$

#### 5.0 Mechanical Description

5.1 Preliminary telescope and MCP detector design is given in Drawing 78000-R-P

##### 5.2 Weight

Each assembly of telescope MCP detector is estimated to weigh 150 kg.\* Additional experiment support equipment (C+DP, harnessing, etc.) is estimated to weigh 30 kg.

##### 5.3 Moving Mechanical Assemblies

Dust covers over telescope entrance annulus released with NSI powered pinpullers.

Vacuum box door on each MCP detector operated by a reversible DC motor.

A sunshade over each detector will close in case of loss of power or loss of spacecraft orientation.

The PC instrument will have a small mechanism to exchange detector units.

##### 5.4 Materials

5.4.1 Only proven or approved materials will be used, including organic compounds meeting the requirements of NASA-SP-R-0022A. All metals will be passivated. The bulk of the instruments will be aluminum 6061-T6 or stainless steel 300 series.

\* Scanner 3 is estimated to weight 175 Kg.

#### 5.4.2 Magnetics

The instruments are not magnetically sensitive. Each MCP telescope will have a magnetic "broom" at the rear of the mirror. The broom will consist of 6 kg of ceramic magnets. The external field is estimated to be less than 1 gauss at 18 inches and less than .1 gauss at 36 inches.

#### 5.5 Ground Handling

Each telescope is dust tight and will be purgable with  $\text{GN}_2$ . Each MCP detector will have a roughing pump port to which our GSE will need access. The PC detector will have an accessible gas port and relief valve.

#### 5.6 Design Criteria and Testing

Criteria and testing will be to recognized and approved NASA standards.

#### 5.7 Telescope Alignment

Initial mounting:  $2^\circ$

After vibration testing:  $\Delta < .5^\circ$

After launch (1g to 0g,  $+20^\circ\text{C}$  to  $\sim -5^\circ\text{C}$ ):  $\Delta < .5^\circ$

On-orbit changes:  $\Delta < .1^\circ$

Star and/or sun sensors with respect to telescopes:  $< .1^\circ$

#### 5.8 Thermal Environment

Electronics:  $-10^\circ\text{C}$  to  $40^\circ\text{C}$  operating

$-30^\circ\text{C}$  to  $60^\circ\text{C}$  survival

Telescope to detectors:  $\Delta < 5^\circ\text{C}$

### 6.0 Electrical Description

6.1 The spacecraft will interface to a central Command and Data Processor (C+DP) box, which will then communicate with each detector. The C+DP will accept commands and power, and will buffer data from each detector to the spacecraft.

## 6.2 Power

+28  $\pm$  4 VDC on multiple buses

Each telescope: electronics	20W
vac-ion pump	10-20W
optics heater	10-50W
detector heater	100W, sunlight only, one detector at a time
DC motor	15W

The electronics are operated whenever science or housekeeping data is required. Vac-ion pump operation is only when the detector box door is closed, which is a ground operation, but may also be done in flight in case of unexpected detector problems. The DC motor opens/closes the detector box door (about 10 seconds per operation, which should occur only once per telescope at the beginning of the mission or as a result of unexpected detector problems). Optics heater operation is only for the early mission optics bake-out. Detector heater operation will occur infrequently in flight.

C+DP:	2W
Star scanner(2):	4W (Ball Model CS201)
Sun sensor:	1W

6.3 Nominal power profile: night 87W  
day 10W

## 6.4 Electrical Interface

The interconnection of instruments, C+DP, and spacecraft is flexible. However, some basic conventions and design rules which we have followed in the past include:

All interface lines between experiment and S/C should have the appropriate isolation. The digital signals are via optical isolators. Analogs are buffered with respect to a reference ground. Bilevels are from isolated



relay contacts. Pulsed commands are to latching magnetic relays. Sensitive signals or high-frequency lines have the appropriate shielding, grounding, and filtering.

All power lines are to isolated DC/DC convertors via shielded twisted pairs. Fault isolation is provided by redundant fuses. The single-point ground convention is observed. All high voltage supplies are with respect to local chassis ground.

## 7.0 Data Handling Requirements

### 7.1 Serial Digital Interface (Redundant)

Output: standard "3-wire" interface, 16 bit words

2 to 10 kbps for each telescope, science data, highly desirable

300 bps, housekeeping data (see 7.2 and 7.3)

10 bps for the star scanners

1 bps for the sun sensor

Input: standard "3-wire" interface, 16 bit words as necessary to command the C+DP box

The format is flexible; NRZ-L, positive logic, TTL compatible logic is satisfactory.

### 7.2 Analogs

The housekeeping analog monitors can be either multiplexed to the S/C TM system, or they can be digitized (8-bits) and inserted into the serial data stream by the C+DP. The analogs will span 0 to 5V. There will be 100 analogs.

Each Telescope:

Suggested Sampling Rate  
1/sec      1/min

Dust cover 1 position	x
Dust cover 2 position	x
Door position	x
Pulse height 1	x

(cont.)	Each Telescope:	Suggested Sampling Rate	
		1/sec	1/min

Pulse height 2	x	
Dead time	x	
Count rate	x	
Discriminator		x
Temp 1		x
Temp 2		x
Temp 3		x
HV 1	x	
HV 2	x	
HV Current 1	x	
HV Current 2	x	
Pump HV		x
Pump Current		x
Heater Current		x
Spare 1		x
Spare 2		x

Additional for the PC Detector:

Pressure 1	x	
Pressure 2	x	
Temp 1		x
Temp 2		x
Valve position 1		x
Valve position 2		x

CP+DP:

Telescope 1 current	x	
Telescope 2 current	x	
Telescope 3 current	x	
Telescope 4 current	x	
C+DP current	x	
Star scanner current	x	
Sun sensor current	x	
Star scanner output	x	
Sun sensor output	x	
Artificial stimulus ramp	x	
Spare 1		x
Spare 2		x
Spare 3		x
Spare 4		x

### 7.3 Bilevels

The housekeeping bilevel monitors can be either multiplexed to the S/C TM system, or they can be buffered and inserted into the serial data stream by the C+DP. The bilevels will be either 0 or Ref volts. There will be 100 bilevels. Suggested sampling rate: 1/minute.

Each Telescope:

Door Enable/Disable  
Door Open/Close  
Discriminator 2/1  
HV 1 On/Off  
HV 2 On/Off  
HV MSB Hi/Lo  
HV LSB Hi/Lo  
Data processor A/B  
Data A switch 2/1  
Data B switch 2/1  
Rate shutdown On/Off  
Heater On/Off  
Pump On/Off  
Quadrant 1 Blanked  
Quadrant 2 Blanked  
Quadrant 3 Blanked  
Quadrant 4 Blanked  
Spare 1  
Spare 2  
Spare 3

Additional for the PC Detector:

Heater 1 On/Off  
Heater 2 On/Off  
Valve 1 Open/Close  
Valve 2 Open/Close

C+DP:

Telescope 1 On/Off  
Telescope 2 On/Off  
Telescope 3 On/Off  
Telescope 4 On/Off  
Sun sensor On/Off  
Star scanner On/Off  
Threshold Hi/Lo  
Artificial Stimulus On/Off  
C+DP On/Reset  
Command Error Yes/No  
Error Reset Yes/No  
Synch Yes/No  
Spare 1  
Spare 2  
Spare 3  
Spare 4

## 8.0 Command System

8.1 Most commands will be by 16-bit word transmitted from the S/C TM system to the C+DP. This will allow great flexibility in commanding the four instruments and in reprogramming the C+DP or troubleshooting. The S/C will be responsible for general power bus control and for the firing of all pinpuller/NSI devices.

In addition, 50 discrete +28V, 100 millisecond pulse commands are required. These go to critical latching relays and will be used in the event of catastrophic failure of the C+DP.

### Each Telescope:

- Door Enable
- Door Open
- HV1 On
- HV1 Off
- HV2 On
- HV2 Off
- Rate shutdown Off
- Heater Off
- Pump Off

### Additional for the PC Detector:

- Heater 1 Off
- Heater 2 Off
- Valve 1 Open
- Valve 2 Close

### C+DP:

- Telescope 1 On
- Telescope 2 On
- Telescope 3 On
- Telescope 4 On
- Sun sensor Off
- Star scanner On
- Artificial stimulus Off
- C+DP Reset
- Error Reset
- Spare

## 8.2 Command Frequency

Nominally experiment commanding will only be done once per civil day. However, commanding every rev may be required during troubleshooting, and during troubleshooting, and during the early days of the mission involving experiment initiation.

## 9.0 Safety

### 9.1 Pyrotechnic Devices

Low energy pyro devices are used on each telescope. Space-qualified pinpullers energized by NASA Standard Initiators (NSI's) are used to release each telescope's dust covers and, in case of failure to open the detector box, to open the sunshade, and to exchange the PC detectors.

### 9.2 Proportional Counter Gas

A space-qualified pressure vessel will contain approximately 1 kg of PC gas, nominally methane, at 1500 psi.

## 10.0 Ground Operations

Full check-out of experiments and S/C systems will be required on the ground during qualification testing, calibration, integration at the S/C contractor, and at the Shuttle launch facility.

No special instrument test or check-out is required once the spacecraft is in the shuttle bay, during launch, or during EUVE orbital insertion.

## 11.0 Post-Launch Operations

### 11.1 Real-time Data

RT scientific data is not required except during the early mission check-out or in the event of failure and troubleshooting is required.

RT housekeeping data is required as the normal part of satellite operations.

#### 11.2 Production Tapes

Computer compatible magnetic tapes with scientific, housekeeping, and aspect data are required. They will be sent to the Principal Investigator for reduction and analysis.